Restructuring Transition Metal Oxide Nanorods for 100% Selectivity in Reduction of Nitric Oxide with Carbon Monoxide

Shiran Zhang[1], Junjun Shan[1], Yuan Zhu[1], Luan Nguyen[1], Weixin Huang[1], Hideto Yoshida[2], Seiji Takeda[2], Franklin (Feng) Tao[1]*

[1]Department of Chemistry and Biochemistry, University of Notre Dame, Notre Dame, Indiana,
46556, USA
[2]Institute of Scientific and Industrial Research, Osaka University, 8-1 Mihogaoka, Ibaraki, Osaka
567-0047, Japan

1. Synthesis of Co_3O_4 nanorods

Cobalt oxide (Co_3O_4) nanorods were synthesized following a modified hydrothermal method reported in literature. The large-scale image (Figure 1a) shows Co_3O_4 has a diameter of ~6 nm with a length of ~100 nm in average. High resolution image (Figure 1b) shows the crystallization of Co_3O_4 phase, supported by XRD pattern (Figure S1b). The measured inter-planar distance, 2.88 Å is consistent with the value of (220) reported in literature[1,2]. It suggests that the preferentially exposed surface is Co_3O_4 (110).

To provide information on the formation of Co_3O_4 nanorods, the growth process is described in the following paragraphs based on literatures [2].

In the synthesis of Co_3O_4 nanorods, cobalt acetate tetrahydrate is used as the synthetic precursor; it undergoes a hydrogenolysis process when dissolved in ethylene glycol due to the considerably large molecular ratio of ethylene glycol to water. In this case, ethylene glycol is regarded as both a simple solvent and a coordination agent. After the introduction of the sodium carbonate solution, the amount of water molecules increases and triggers hydrolysis along with the attendant fast nucleation of the precursors. The precursors then form layered structures with edge-sharing coordination of hydroxide anions, analogous to the layered double hydroxides, which further form sheet-like structures by self-assembly due to the interlaying hydrogen bonds between the acetates and the hydroxides.
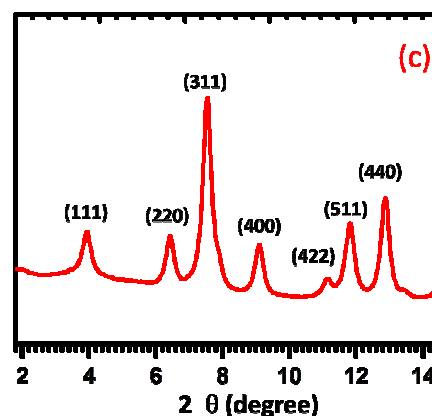

Figure S1 XRD of as-synthesized Co_3O_4 nanorod.

The next step is a direct ion exchange of acetates and hydroxides by carbonate anions that are more strongly held in the interlayers than the monovalent anions[4]. This leads to a dissolution-recrystallization process in which carbonate anions dissolve the layered structures by replacing the acetates and hydroxides. Carbonate anions also serve as the structure-directing agent; that is, they attack and coordinate with the Co^{2+} to crumple the sheets. As there are more Co^{2+} in the (110) plane, the recrystallization will be inhibited by the coordination of Co^{2+} to carbonate anions, which gives rise to the preferential exposure of (110) plane. It is believed that the carbonates are prone to attacking the defects of the sheets and further disrupt the whole structure.

In the aging stage, ethylene glycol is incorporated into the structure by replacing both carbonates and acetates. Ethylene glycol largely influences crystalline aggregation and promotes formation of a network of small interconnected pores. It further contributes to the disintegration of the remaining sheet-like structures and fulfills the formation of pristine nanorods in solution. The pristine nanorods are then washed with deionized water and ethanol and then calcined at $250^{o}C$-$350^{o}C$ in air for 4 hours. In the calcination, most of carbon species introduced in synthesis were removed through combustion to CO_2 and H_2O.
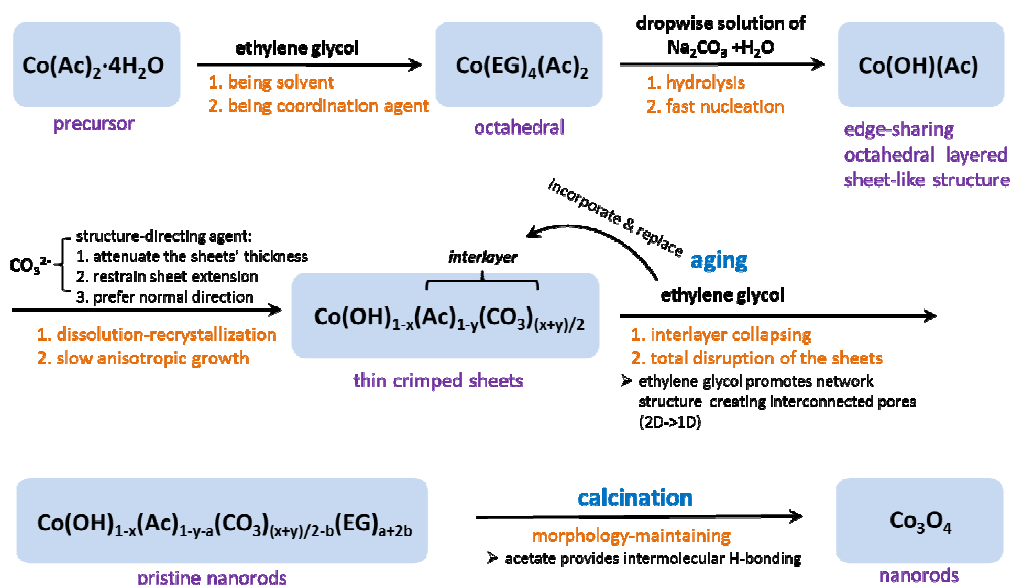

Figure S2 Schematic showing the formation of nanorod morphology in the growth of Co₃O₄ nanorods.

2. Measurements of catalytic activity and selectivity

Measurements of catalytic activity and selectivity in reduction of NO with CO were performed in a micro fix-bed flow reactor. Gas chromatograph analyzed gases from this reactor under different reaction conditions. Two pre-mixed gas cylinders were used. The mixed gas in one cylinder is 15% CO + 5% NO + 80 % Ar, the other is 15% CO + 15% NO + 70% Ar. Certain amount of catalysts was loaded into the micro reactor. Conversion and selectivity were calculated with:

Conversion of nitric oxide $= \frac{[total\ nitric\ oxide\ introduced\ to\ reactor]-[unreacted\ nitric\ oxide]}{[total\ nitric\ oxide\ introduced\ to\ reactor]} \times$ 100%

Selectivity to production of nitrogen $= \frac{[produced\ nitrogen]x\ 2}{[total\ reacted\ nitric\ oxide\ ]} \times 100\%$

Selectivity to production of nitrous oxide $= \frac{[produced\ nitrous\ oxide]x\ 2}{[total\ reacted\ nitric\ oxide\ ]} \times 100\%$

3. Calculation of turn-over frequency

Turn-over frequency (TOF) was calculated by using the measured conversion of 10 mg Co_3O_4 catalyst. We assume all the oxygen atoms of the surface lattice of CoO are active in the production of N_2 and that the average dimensions of the nanorods are 6 nm×6 nm×100 nm.

(a) Calculation of the total surface area of 0.01 g of Co_3O_4 nanorods

(a1) Volume of 10 mg of Co_3O_4 nanorods (the average size of nanorods is 6 nm × 6 nm × 100 nm based on TEM):

Figure S3 Schematic of a Co_3O_4 nanorod (6nm × 6nm × 100nm).

0.01g / 6.11 g/cm^3 = 1.64 × 10^{-3} cm^3 = 1.64 × 10^{18} nm^3

(a2) Volume of a single anorod (6 nm × 6 nm × 100 nm): V_o=3,600 nm^3

(a3) Total number of nanorods in 0.01 g of Co_3O_4 nanorods (6 nm×6 nm×100 nm)

$N_{nanorods}$ = V_{total} /$V_{each\ nanorod}$ = 4.556 × 10^{14}

(a4) Surface area of a nanorod (6 nm × 6 nm × 100 nm) (see Figure S3):

Two (1-10) surfaces: 6 nm × 100 nm × 2 = 1200 nm^2
Two (001) surfaces: 6 nm × 100 nm × 2 = 1200 nm^2
Two (110) surfaces: 6 nm × 6 nm × 2 = 72 nm^2
Total surface area of a nanorod: 2472 nm^2

(a5) Total surface area of 10 mg of Co_3O_4 nanorods:

Total (1-10) surface of all nanorods:
$N_{nanorods}$ × $A_{two\ (1-10)\ surface\ of\ each\ nanorod}$ = 5.467 × 10^{17} nm^2
Total (001) surface of all nanorods:
$N_{nanorods}$ × $A_{two\ (001)\ surface\ of\ each\ nanorod}$ = 5.467 × 10^{17} nm^2
Total (110) surface of all nanorods:

$$N_{\text{nanorods}} \times A_{\text{two (110) surface of each nanorod}} = 3.28 \times 10^{16} \text{ nm}^2$$

(b) Total number of cobalt ions on the surfaces of all Co_3O_4 nanorods (0.01 g)

There are two kinds of terminations for Co_3O_4 (1-10): *types A* and *B*. *Type A* has both Co^{2+} and Co^{3+} while *type B* has only Co^{3+} ions. We preferentially consider *type B* as the exposed (1-10) surface of Co_3O_4 nanorods for catalysis as Co^{3+} exhibits a higher binding energy to CO[1]. Here the TOF calculation was performed on *type B* surface of Co_3O_4 (1-10).
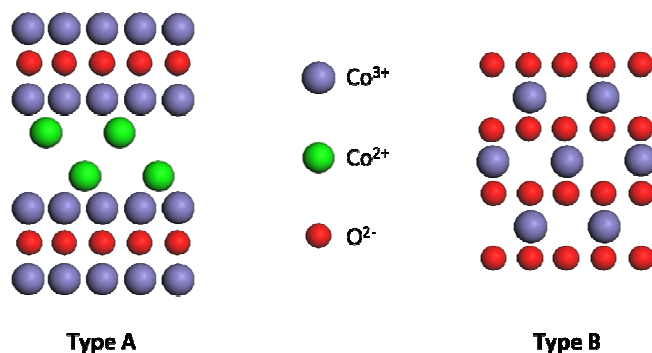

Figure S4 Schematic of types A and B surface of Co_3O_4 (1-10).

Figure S4 shows the size of a 2-D surface unit cell of type B surface of Co_3O_4 (1-10). For (1-10) and (001) surfaces (Figure S5), each square nanometer (1 nm^2) has 5 ions and 6.12 ions of Co^{3+}, respectively [5]. By considering the surface areas of (1-10), (001), and (110) calculated in (a5), the number of Co^{3+} ions on the nanorod surface should be

Figure S5 Surface structural parameters of type B surface of Co_3O_4 (1-10) (a) and Co_3O_4 (001)(b).
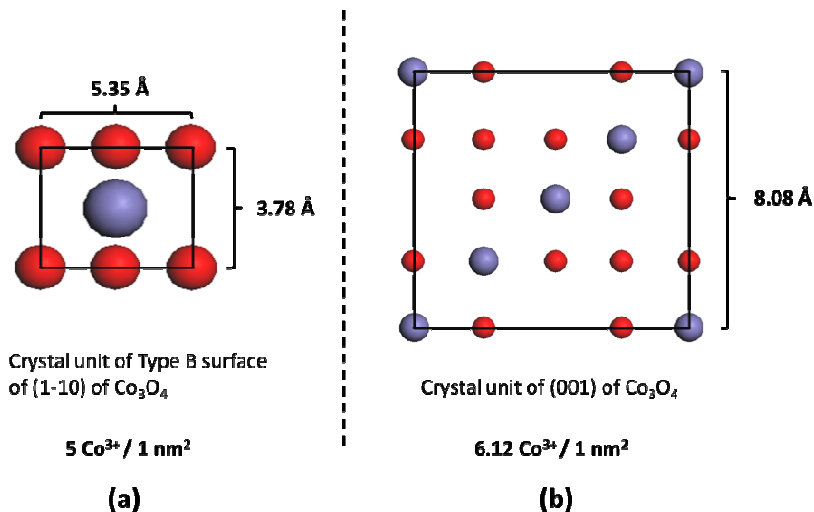
$$N(Co^{3+}) = 5 \times 5.467 \times 10^{17} + 6.12 \times 5.467 \times 10^{17} + 5 \times 3.28 \times 10^{16} = 6.24 \times 10^{18}.$$

That is, there are approximately 6.24×10^{18} Co^{3+} ions on the surface of 10 mg of Co_3O_4 nanorods. We assume that this number of cobalt ions does not change after chemical reduction from Co_3O_4 to CoO. Thus the total number of Co^{2+} ions (the active phase of CO+NO at high temperatures) of CoO is 6.24×10^{18}.

(c) Turn-over-frequency for production of N_2 on the non-stoichiometric cobalt oxide

In order to calculate the TOF, we measured the catalytic performance by loading 10 mg of as-synthesized Co_3O_4 nanorods. The flow rate was tuned to have catalysis in kinetics control regime (the conversion rate of NO was controlled at ≤10%). The number of nitric oxide molecules passing through the catalyst each second was calculated. Based on the number of the converted molecules of nitric oxide per second and the calculated number of cobalt ions on surface of 10 mg of nanorods, TOF was calculated. It is 0.08 N_2 molecules per second per Co^{3+}.

4. Ambient pressure X-ray photoelectron spectroscopy and in-situ studies of surface chemistry of catalysts during catalysis and under reaction conditions
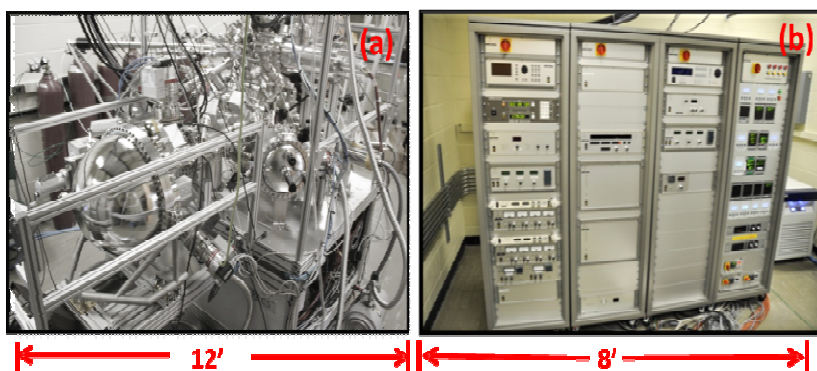

Figure S6 Represented photos of the ambient pressure XPS (AP-XPS) system in Tao group[3]. (a) In-house AP-XPS using monochromatic Al Kα; (b) Control system of the in-house AP-XPS.

Use of electron spectroscopy to study materials surface was launched decades ago[6,7]. The first synchrotron-based ambient pressure XPS (AP-XPS) was designed by a team of Berkeley Scientists led by Miquel Salmeron in 2002 [8].

We used an in-house AP-XPS using monochromatic Al Kα (Figure S6) available in our group. The collection of photoelectrons from surface embedded in gas phase is based on differential pumping stage installed on energy analyzer which was early developed in 2002[8,9]. Figure S7 schematically shows the setup of a differential pumping system[6,11]. This system has a catalytic reactor. The introduced reactant gases flow through the catalyst surface. Products and the left reactant gases are flowing out through an exit. The sample can be heated to different temperatures when the sample is in gaseous environments with different pressures. Acquisition time of each spectrum of Co 2p in Figure 1a is only about five minutes because the concentration of cobalt in catalysts is quite high. It is noted that we didn't find any potential reduction of Co_3O_4 or CoO induced by Al Kα irradiation even Co_3O_4 and CoO samples were scanned for two hours continually.
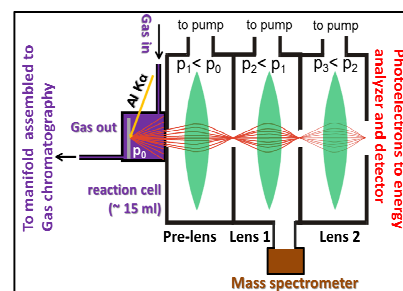

Figure S7 Schematic of differential pumping for collection of photoelectrons from a surface embedded in gas environment.[6,7,8,11]

5. Photoemission features of Co_3O_4 and CoO_{1-x}

Figure S8 and S9 are the deconvoluted spectra of Co_3O_4 and CoO_{1-x}, respectively. Obviously, the satellite peaks of Co 2p of Co_3O_4 (Figure S8) appeared at higher binding energy with much lower intensity in contrast to those of CoO_{1-x} (Figure S9).
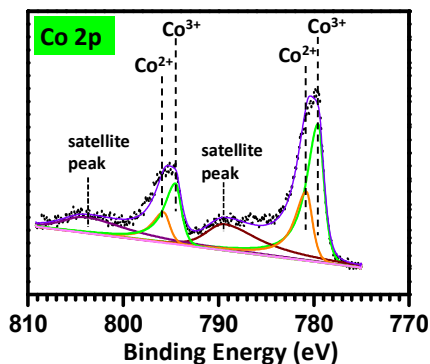

Figure S8 Deconvoluted spectrum of Co 2p of Co_3O_4 at room temperature (before reaction).
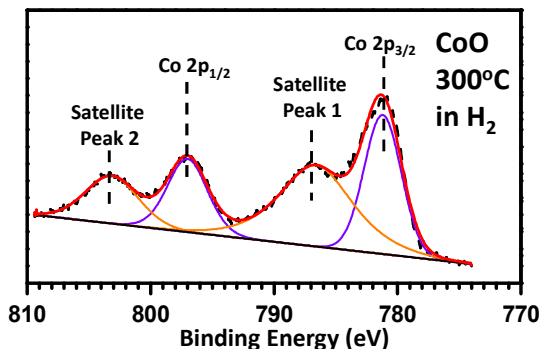
Figure S9 Devonvolution of Co 2p of CoO_{1-x} formed at 300^oC in H_2.

6. Restructuring of Co_3O_4 nanorods in different gases

Co_3O_4 nanorods can be reduced to CoO_{1-x} in pure CO and pure H_2 other than reactant mixture of CO and NO (Figure 2). Figure S10a and Figure S10b show the photoemission features of Co 2p collected when Co_3O_4 is in pure CO at 0.3 Torr or H_2 at 0.1 Torr at different temperatures, respectively. As the photoemission feature of Co 2p3/2 and Co 2p1/2 of Co^{2+} at the octahedral sites of rocksalt CoO_{1-x} exhibits characteristic satellite peaks at 786.4 eV and 803.1 eV, reduction of Co_3O_4 to CoO_{1-x} in reducing in-environments can be tracked through in-situ observation of the appearance of these characteristic satellite peaks. Figure S10a and Figure S10b clearly show the progressive reduction of Co_3O_4 nanorods to CoO_{1-x} in CO or H_2, respectively. Figure S10c presents surface chemistry of Co_3O_4 catalyst in pure NO at different temperature. There is no reduction at a temperature lower than 350^oC. At 400^oC, Co_3O_4 is decomposed to CoO.

Figure S9 is a spectrum of Co 2p of Co^{2+} in octahedral coordination with oxygen atoms in CoO. It has better signal-to-noise ratio due to more scan times. The characteristic satellite peaks of CoO are marked in Figure S9. Obviously, there is no such satellite peaks in the Co 2p of Co_3O_4 nanorods (See Figure S8).
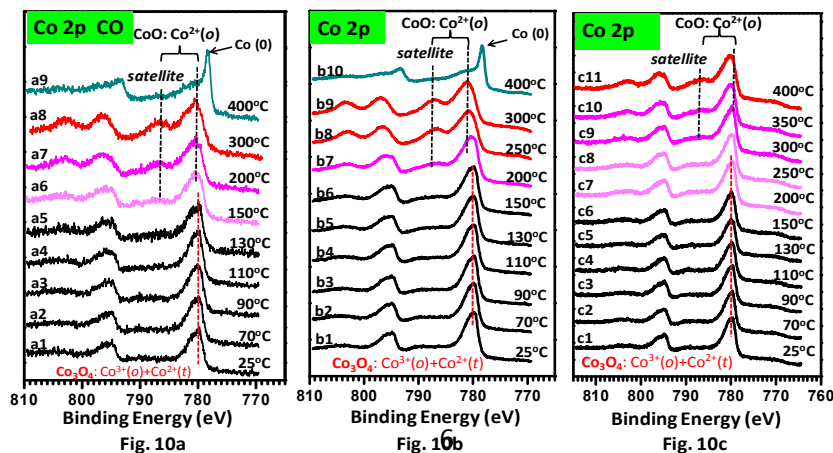

Fig. 10a

Fig. 10b

Fig. 10c

Figure S10. Photoemission features of Co 2p of Co_3O_4 in different reactant gases. (a) in pure CO (0.3 Torr). (b) in pure H2 (0.3 Torr). (c) in pure NO.

7. Catalytic performances in reactant mixture with different gas compositions

Figure S11 presents the catalytic performance of cobalt oxides in a gas mixture composed of CO (15%), NO (15%), and Ar (70%) in the temperature range of 50^oC-440^oC. At 400^oC, the selectivity of N_2 is 98%. It reaches 100% at 420^oC and 440^oC. This catalytic performance is very similar to that in a gas mixture with composition of CO (15%), NO (5%), and Ar (80%) in 50-480^oC (Figure 4). The close similarity of catalytic performance in reactants with CO:NO of 1:1 to 3:1 (Figure S11 and Figure 4) is supported by the same surface chemistry of CoO identified with AP-XPS at 3 Torr NO and 3 Torr CO (Figure S12) and 1 Torr NO and 3 Torr CO (Figure 2).
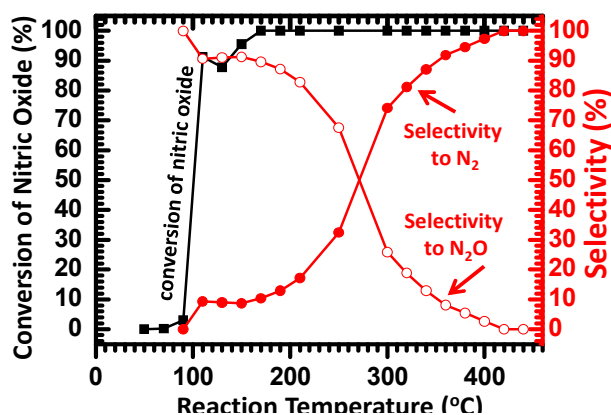

Figure S11 Catalytic activity and selectivity of a nominal structure cobalt oxide at different temperatures (50^oC-440^oC) in the mixture gas of CO (15%) and NO (15%).
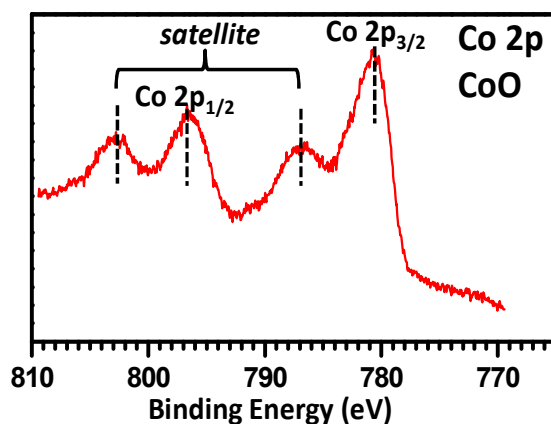

Figure S12 Co2p of CoO formed at 420^oC in 3 Torr CO and 3 Torr NO.

8. Catalytic conversion of CO

Figure S13 presents the conversion of CO at different temperature of catalysis of NO reduction with CO on Co_3O_4. As molar ratio of CO to NO is 3:1, 33±1% CO is converted when NO is fully reduced to N_2 based on the stiochiometric ratio: $2CO+2NO=N_2+CO_2$.
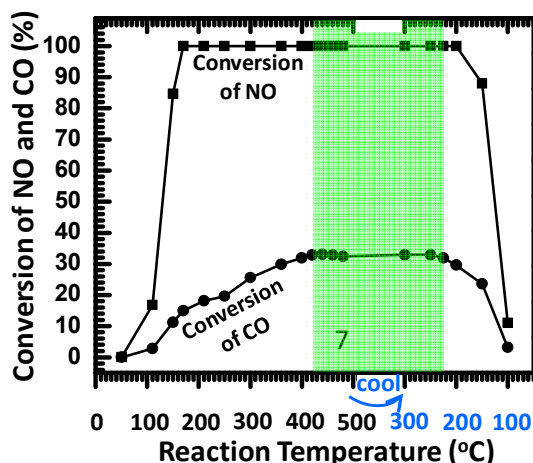
Figure S13 Conversion of CO and NO on Co3O4 at different temperature in the mixture of reactants of CO and NO (pressure ratio of CO to NO=3:1)

9. AP-XPS studies of cobalt oxide in reactant mixture with different compositions

To investigate the possible influence of the gas composition on the surface chemistry of a catalyst, AP-XPS was used to study the cobalt oxide catalysts in mixture of CO and NO with different compositions. Figure S12 presents a representative spectrum of Co 2p photoemission of CoO_{1-x} under a reaction condition of 420^oC in 3 Torr CO and 3 Torr NO (ratio of 1:1). Compared to the mixture of 1 Torr NO and 3 Torr CO in Figure 2, CoO at 420^oC in 3 Torr CO and 3 Torr NO (Figure S12) exhibits the same surface chemistry. The same surface chemistry of catalysts in reactant gases with compositions of 3:1 (Figure 2 and S14) and 1:1 (Figure S12), is consistent with the very similar catalytic performance on CoO at 420^oC in mixture of CO and NO with different gas compositions (Figure 4 for 3:1 and Figure S11 for 1:1).
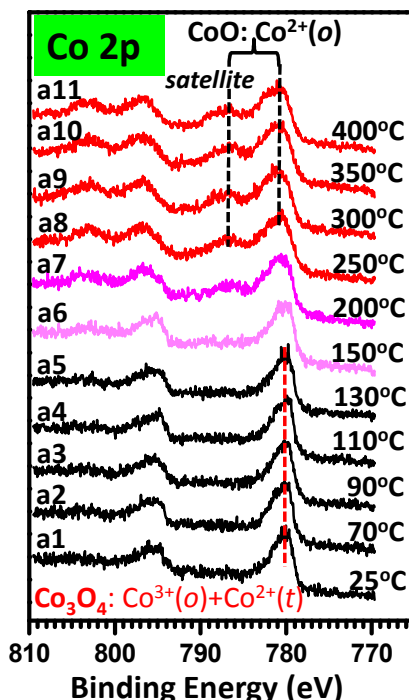
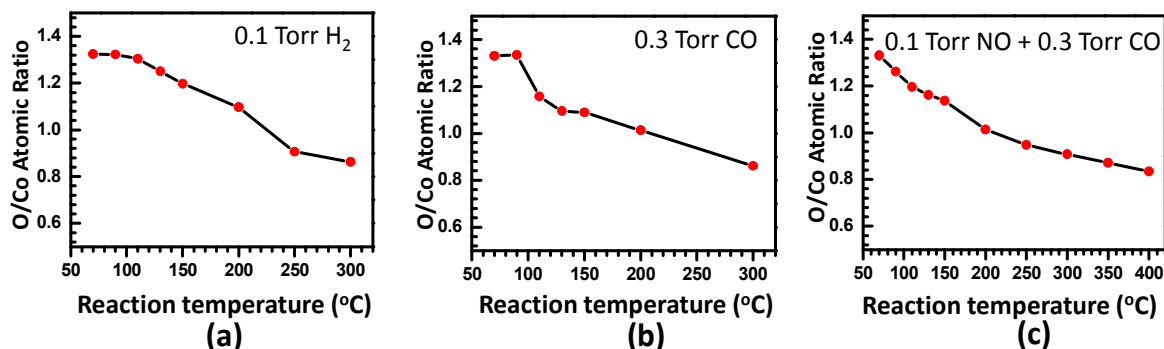*Figure S14. Co 2p of cobalt oxide in a mixture of 0.3 Torr CO and 0.1 Torr NO.*

Figure S15. Atomic ratio of oxygen to cobalt atoms in different reactive gaseous environments.

10. Oxygen vacancies on the surface of CoO_{1-x}

8

Oxygen vacancies are important structural defects for reducible oxides. The O/Co atomic ratios of cobalt oxides at different temperatures were calculated with the following method based on AP-XPS data. First, the area ratio of O 1s to Co 2p of Co_3O_4 at room temperature was calculated. A factor can be obtained by using the area ratio of O 1s to Co 2p to divide the stoichiometric ratio of O to Co in Co_3O_4, 4/3. Oxygen vacancies on Co_3O_4 during calcination in preparation of Co_3O_4 nanorods (an experimental step in preparation of Co_3O_4 nanorods) could be generated since oxygen atoms likely lose at high temperature. Notably, in the process of cooling down to room temperature in air, H_2O molecules in air typically adsorb and dissociate on oxygen vacancies to form OH groups which fill in oxygen vacancies. Therefore, the number of oxygen atoms of surface is almost identical to that of a stoichiometric surface of Co_3O_4 (O/Co=1.33). Thus, we prefer to consider the O/Co ratio of CO_3O_4 at room temperature is to be1.33 since OH groups fill into oxygen vacancies.

Dividing the area ratio (A_{O1s}/A_{Co2p}) at a temperature by this factor gives the atomic ratio of O/Co at this temperature. Interestingly, the atomic ratios of oxygen to cobalt of CoO_{1-x} formed at 300^oC in H_2, 300^oC in CO, at 400^oC in CO+NO are 0.86, 0.84, and 0.82, respectively (Figure S15a, Figure S15b, and Figure S15c) instead of the stoichiometric ratio of CoO. A similar ratio, 0.78 was identified for CoO at 400^oC in the gaseous mixture of 1 Torr NO and 3 Torr CO (Figure 6). These ratios suggest the existence of nonstoichiometric CoO_{1-x} in the mixture of CO and NO under reaction conditions. In addition, there is no a significant difference in the O/Co ratio between two different pressure regimes (0.4 Torr of CO+NO in Figure S15c versus 4 Torr of CO+NO in Figure 6).

11. AP-XPS studies of cobalt oxide in reactant mixture of CO and NO with different pressures

We examined the surface chemistry of CoO_{1-x} in a mixture of 3 Torr NO and 3 Torr CO (Figure S12). Although the total pressure of 6 Torr in Figure S12 is 15 times higher than 0.4 Torr in Figure S14a11, there is no obvious difference in the surface chemistry of the catalysts under reaction conditions. Thus, we deduce that there is no obvious difference in surface chemistry of catalysts *between* the Torr pressure range of AP-XPS studies (Figure 2, S12, and S14a11) *and* 38 Torr (5% NO in reactor; 5% × 760 Torr = 38 Torr at which we measured catalytic activity and selectivity of the catalyst in a micro fixed-bed flow reactor using gas chromatography).

12. Representation of the origin of satellite peaks of Co^{3+} of Co_3O_4 and Co^{2+} of CoO

The spectrum of Co 2p of Co_3O_4 at room temperature was fitted with asymmetric main peaks and satellite peaks (attributable to Co^{3+} of Co_3O_4 at 789.6 eV) upon a subtraction of a linear background (Figure S8). Each main peaks (Co $2p_{3/2}$ or Co $2p_{1/2}$) was deconvoluted into Co^{3+} and Co^{2+} peaks with an approximate area ratio of 2 to 1, which is consistent with the crystallography of Co_3O_4.

Kim demonstrated that these shake-up satellite peaks originate from the effects of monopole charge-transfer transitions from O 2p e_g to Co 3d e_g, accompanying the primary photoionization process[10]. In order for an efficient charge-transfer transition, the crystal system should have a strong electron coupling effect. This effect is much more significant in an octahedral configuration of cobalt cations, like Co^{3+} in Co_3O_4 (BE=789.6 eV for Co^{3+} in spinel Co_3O_4 in Figure S8), or Co^{2+} in CoO (BE=786.4 eV for Co^{2+} in rock-salt CoO_{1-x} in Figure S9) which contain a single electron after the crystal splitting of its 3d orbitals.

13. Potential reaction mechanisms for nitric oxide reduction with carbon monoxide on cobalt oxides

Co_3O_4 nanorods exhibit activity in catalyzing CO+NO at a temperature as low as 110°C and can attain 100% conversion of NO at 170°C with selectivity of 8% to production of N_2. Both AP-XPS and E-TEM showed the preservation of Co_3O_4 phase at temperatures lower than 200°C. The potential catalytic mechanic pathways of CO+NO on Co_3O_4 and CoO are discussed in the following sections. We expect theoretical calculation will be necessary for revealing catalytic mechanism of reduction of NO with CO on the two different oxide catalysts.

(a) Potential paths to form N_2O and N_2 in reduction of NO with CO on Co_3O_4

The preferentially exposed surface from TEM studies is the (110) surface of Co_3O_4 (Figure 1b). We selected B-type surface as the exposed surface[11]. There are two types of oxygen atoms, O_{2f} and O_{3f} which coordinate with two and three oxygen atoms, respectively (Figure S16).

Figure S17 schematically presents the formation of N_2O on Co_3O_4 nanorods. A CO molecule adsorbs on an O_{2f} atom (Figure S17b). Due to the high capability of Co_3O_4 in releasing oxygen atoms, each CO molecule binds to an O_{2f} atom and weakens the interaction between O_{2f} and a Co^{3+}, forming a CO_2 molecule (Figure S17b). The following desorption of the formed CO_2 molecule produces an oxygen vacancy (Figure S17c). This oxygen vacancy can adsorb a nitric oxide molecule (Figure S17d). Another nitric oxide molecule can weakly adsorb on a Co^{3+} ion adjacent to the oxygen vacancy just filled with the first NO molecule (Figure S17e). The strong interaction between a Co ion and an oxygen atom of the NO molecule and the coupling between nitrogen atoms of these two adjacent nitric oxide molecules (Figure S17f) largely weakens the N-O bond of nitric oxide. The coupling between the weakly bonded *nitrogen atom* to oxygen atom and the *nitric oxide molecule* weakly binding to Co^{3+} forms a N_2O molecule (Figure S17f). Desorption of the N_2O molecule restores the clean surface of Co_3O_4 (Figure S17a) which is ready for the next cycle. The overall reaction of one catalytic cycle can be
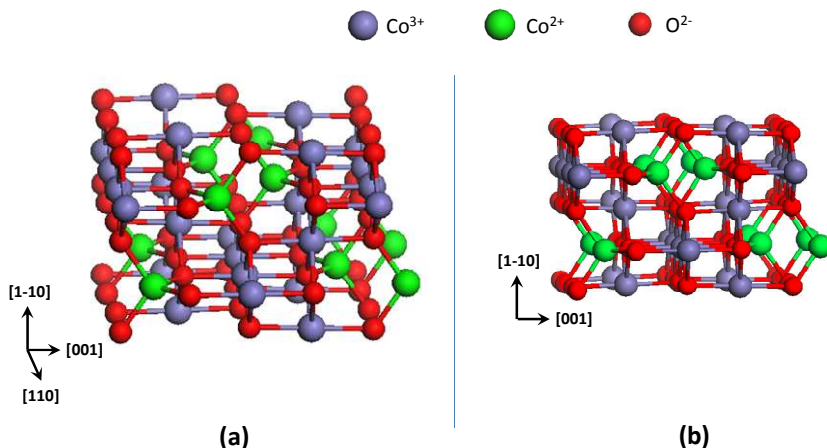

Figure S16 Schematic of Co_3O_4 with B-type (1-10) surface. (a) View at 45° between [110] and [1-10]. (b) View from [110] (side view).

represented as $CO + 2NO \rightarrow CO_2 + N_2O$.

In terms of N_2 production by reducing NO with CO on Co_3O_4, two CO molecules are adsorbed on two O_{2f} atoms (Figure S18b) and go on to form two CO_2 molecules. Desorption of CO_2 molecules creates two oxygen vacancies (Figure S18c). A recent calculation of CO oxidation on Co_3O_4 showed the barrier for hopping an O_{2f} atom to its adjacent oxygen vacancy is quite low [11]. If this hopping event should happen, a pair of oxygen vacancies would form (Figure S18d). Then, two nitric oxide molecules will adsorb at the two adjacent vacancies and thus strongly bond to the adjacent Co^{3+} ions (Figure S18e). The two nitrogen atoms of the two adjacent NO molecules bonded to vacancies can couple together (Figure S18f). The coupling between two nitrogen atoms of two adjacent nitric oxide molecules and the strong binding of oxygen atoms of nitric oxide to Co^{3+} ions, largely weaken the N-O bonds of nitric oxide molecules. The two nitrogen atoms of the two adjacent bonded NO molecules form a nitrogen molecule (Figure S18f). Desorption of the nitrogen molecule restores a clean Co_3O_4 surface (Figure S18a), which is ready for catalysis of the next cycle.

Notably, the mechanism of N_2 production involves the hopping of an oxygen atom to its adjacent oxygen vacancy (Figure S18c and Figure S18d). Thus, it is expected that a high temperature is favorable for the formation of N_2 since more hopping events occur at a higher temperature from the point of view of thermodynamics. Thus, it is expected that production of N_2 is favorable at high temperature but N_2O at low temperature, which is consistent with what we observed for Co_3O_4 in Figure 3. The above mechanism can rationalize the observed increase in N_2 selectivity at higher temperature (Figure 4).

(b) Potential paths to form N_2 and N_2O in reduction of NO with CO on CoO

Figure S19 presents the atomic arrangement on CoO(1-10). Figure S20 schematically presents the formation of N_2 by reducing NO with CO on CoO, respectively. Two CO molecules can adsorb on two surface lattice oxygen atoms of CoO (1-10) (Figure S20b1 or Figure S20b2). By weakening the two Co-O bonds, two CO_2 molecules can form. Once CO_2 molecules desorb, oxygen vacancies are created (Figure S20c or Figure S20d). In fact, a *pair* of two *adjacent* oxygen vacancies can be formed
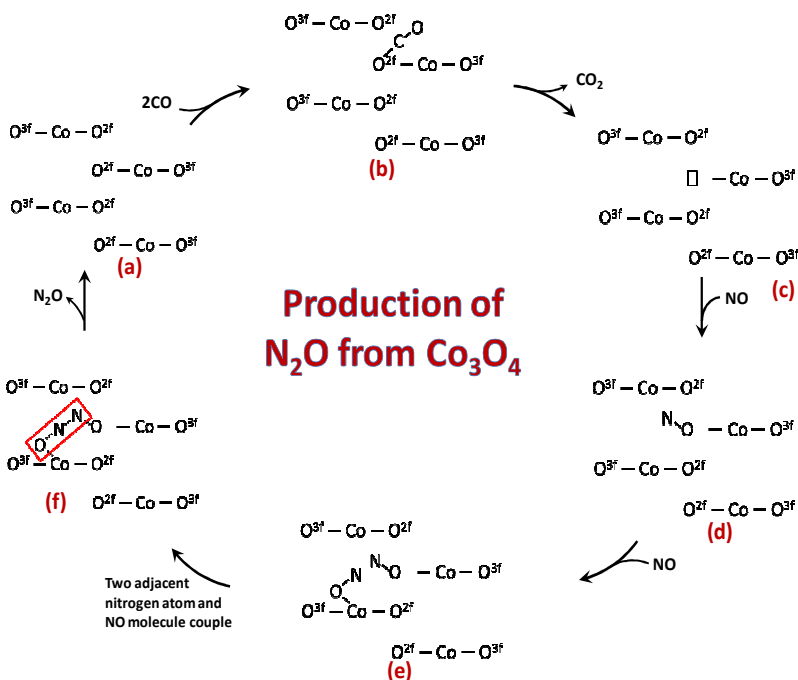

Figure S17 Potential path to form N_2O in reduction of NO with CO on Co_3O_4 (1-10).

through two potential channels: First, by adsorption of two CO molecules on two adjacent

oxygen atoms and a following desorption of two CO_2 molecules (Figure S20b1 and Figure S20d); The other route is by hopping of oxygen vacancies (Figure S20b2, Figure S20c, and Figure S20d)

A part of adjacent oxygen vacancies can be filled by adsorption of nitric oxide molecules (Figure S20e). The strong binding of oxygen atoms of nitric oxide molecules to oxygen vacancies can significantly weaken the N-O bond strength (Figure S20e and Figure S20f). The coupling of nitrogen atoms of the two adjacent nitric oxide molecules further decreases the bond strength of N-O (Figure S20f). Eventually, the dissociation of the two adjacent NO molecules will form a nitrogen molecule (Figure S20f).

Figure S18 Potential path to form N_2 in reduction of NO with CO on Co_3O_4 (1-10).

Notably, the nitrogen atom of NO on an oxygen vacancy (Figure S21e or Figure S20d) could interact with a nitric oxide molecule that is weakly adsorbed on Co^{2+} ion (Figure S21e). This interaction could form a N_2O molecule (Figure S21f). When oxygen vacancy density on the CoO surface is small, the fraction of pairs of oxygen vacancies in all the oxygen vacancies on a CoO surface is low. Thus, the chance of coupling two adjacent NO molecules along [110] is low. As higher temperature is favorable for hopping oxygen atoms along the row of oxygen atoms at [110], the fraction of pairs of oxygen vacancies is high. The chance of coupling nitrogen atoms of two adjacent nitric oxide molecules to form a N_2 molecule is increased. Thus, the N_2 selectivity is increased at high temperature. In addition, a high temperature is favorable for the generation of oxygen vacancies [12,13]; high overall density of oxygen vacancies will certainly increase the ratio of pairs of oxygen vacancies, which is responsible for the production of nitrogen molecules.

These are potential reaction pathway. Theoretical simulation will be significant in identifying reaction pathways on these catalysts.
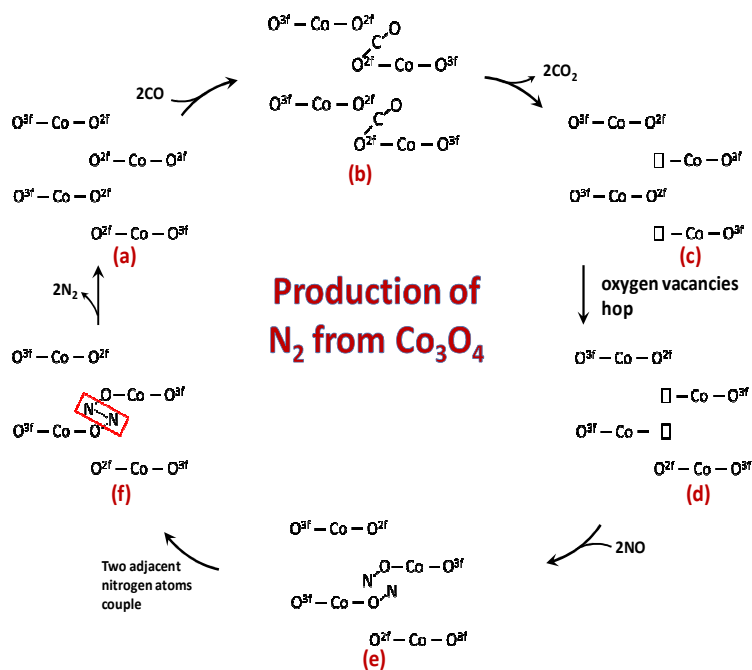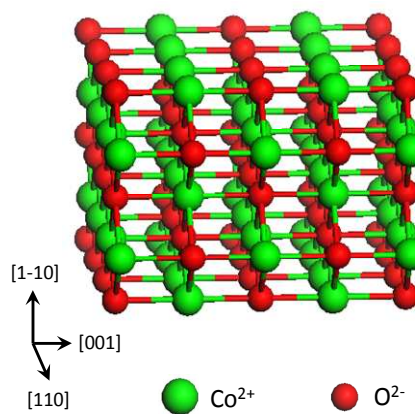
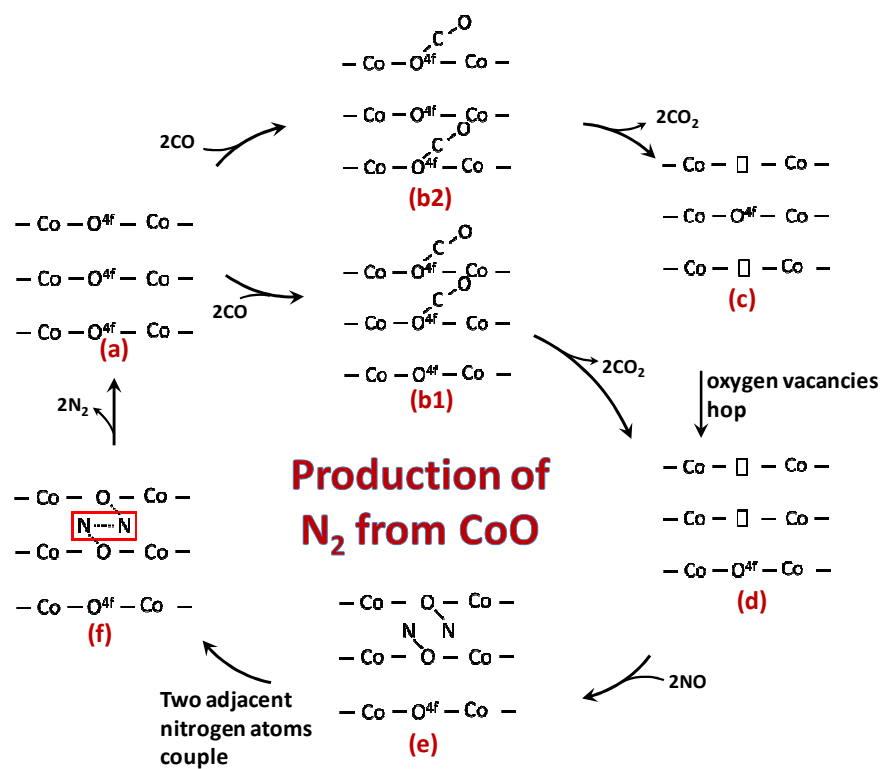*Figure S19 Schematic of CoO surface (1-10)*

Figure S20 Potential path to form N₂O in reduction of NO with CO on CoO (1-10).
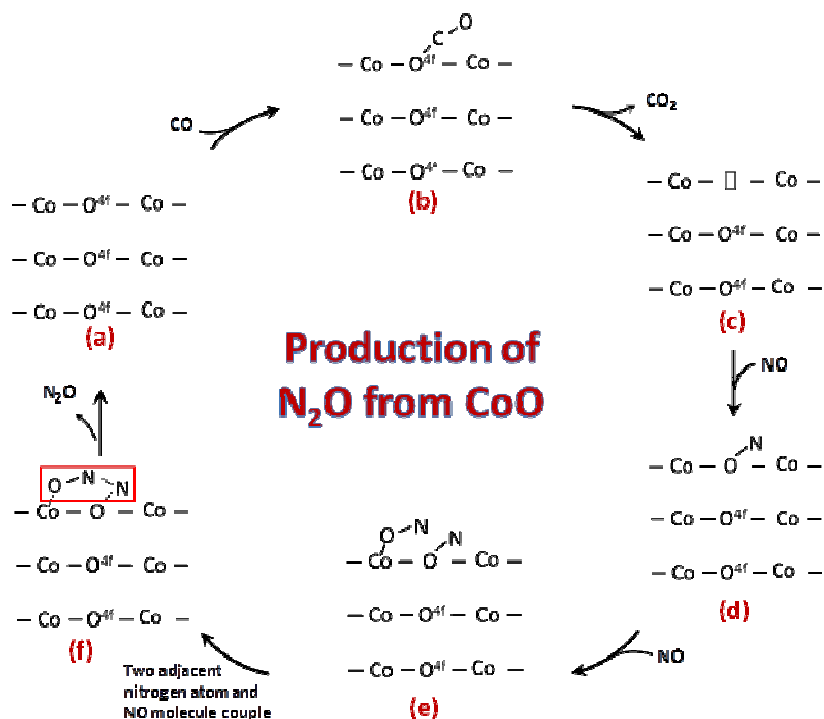
Figure S21 Potential path to form N₂O in reduction of NO with CO on CoO (1-10).

References

(1)   Xie, X.; Li, Y.; Liu, Z.-Q.; Haruta, M.; Shen, W. *Nature* **2009**, *458*, 746.

(2)   Xie, X.; Shang, P.; Liu, Z.; Lv, Y.; Li, Y.; Shen, W. *Journal of Physical Chemistry C* **2010**, *114*, 2116.

(3)   Tao, F. *Chemical Communications* **2012**, *48*, 3812.

(4)   Carlino, S. *Solid State Ionics* **1997**, *98*, 73.

(5)   Smith, W. L.; Hobson, A. D. *Acta Crystallographica Section B-Structural Science* **1973**, *B 29*, 362.

(6)   Lindberg, B.; Asplund, L.; Fellnerfeldegg, H.; Kelfve, P.; Siegbahn, H.; Siegbahn, K. *Chemical Physics Letters* **1976**, *39*, 8.

(7)   Joyner, R. W.; Roberts, M. W.; Yates, K. *Surface Science* **1979**, *87*, 501.

(8)   Ogletree, D. F.; Bluhm, H.; Lebedev, G.; Fadley, C. S.; Hussain, Z.; Salmeron, M. *Review of Scientific Instruments* **2002**, *73*, 3872.

(9)   Salmeron, M.; Schlogl, R. *Surface Science Reports* **2008**, *63*, 169.

(10)   Kim, K. S. *Physical Review B* **1975**, *11*, 2177.

(11)   Jiang, D.-e.; Dai, S. *Physical Chemistry Chemical Physics* **2011**, *13*, 978.

(12)   Esch, F.; Fabris, S.; Zhou, L.; Montini, T.; Africh, C.; Fornasiero, P.; Comelli, G.; Rosei, R. *Science* **2005**, *309*, 752.

(13)   Campbell, C. T.; Peden, C. H. F. *Science* **2005**, *309*, 713.